Arabian Journal of Geosciences (2020) 13:530
https://doi.org/10.1007/s12517-020-05470-z

ORIGINAL PAPER

Analysis, monitoring and simulation of dust hazard phenomenon in the northern Persian Gulf, Iran, Middle East

Mohamadhasan Yazdani[1] · Behrouz Sobhani[2] · Vahid Safarian Zengir[2] · Ata Ghaffari Gilandeh[1]

Received: 3 June 2019 / Accepted: 20 May 2020

Abstract

Dust is a particulate matter in the atmosphere that is created by natural and human agents. Dust has negative effects on various parts of human life, including agriculture, health and economics. In recent decades, in various areas with a lack of rainfall and drought being contested, dust has happened there. One of these areas is the northern part of the Persian Gulf in Iran which has been exposed to dust in recent years. The purpose of the present study was to evaluate and predict the hazardous phenomenon of dust in the western strip of Iran. Therefore, the data of dust from 14 synoptic stations of the study area (1990–2018) using panel data-hybrid neural network and adaptive neuro-fuzzy inference system (ANFIS) models were used. Finally, TOPSIS and simple additive weighting (SAW) multi-criteria decision-making (MCDM) models were used to prioritize more dust-prone areas. The results showed that the reliability of the panel data-hybrid neural network error estimation models is more than the ANFIS. Based on prediction models, the highest probability of occurrence of the maximum dust in the future was observed at Sarpol-e Zahab and Abadan stations (128.917 and 120.709%, respectively). According to the SAW model, the highest probability of occurrence of dust was at Abadan station (998%) and based on the TOPSIS model, Eslamabad-e Gharb, with 997%. It is necessary the inter-organizational cooperation by contracting an international memorandum with neighbouring countries in addition to domestic actions to reduce the damage caused by the dust phenomenon in the study area.

Keywords Natural hazards · Artificial neural network · Dust · Environment · Iran

Introduction

Dust phenomenon is one of the most damaging natural disasters in the world's low rainfall areas, causing many environmental problems in these areas (Khoshkiysh et al. 2012; Xinghua et al. 2019). Like the country, Kuwait is an arid country with an extremely high level of dust loading (Aba et al. 2016). In arid and semi-arid regions, dust storms are a common phenomenon (Ahmed et al. 2016). Correlation between the occurrence of respiratory and cardiovascular diseases and dust storms showed that PM_{10} concentrations were significantly correlated with bronchial (Al-Hemoud et al. 2018). Dust is one of the most dangerous climatic phenomena in the world that annually causes damage to the environment, roads and buildings and urban air. Dust is evaluated with other atmospheric pollutants as a pollutant (Zolfaghari et al. 2011; Aarons et al. 2019). Dust storms are a major factor in the loss of soils and the economic losses to industrial, agricultural and communications sectors in most regions of Iran, especially in the west and southwest, and can threaten human life in terms of health and food production (Dastcherdi et al. 2011; Kasey et al. 2019). Dust is one of the

This article is the product of the authors' original results and all of them are familiar with the publication of the *Journal of Environmental Sciences Europe*. This article has not been published yet in another magazine and is currently not being judged in any magazine.

Responsible Editor: Ali Al-Dousari

✉ Vahid Safarian Zengir
V.Safarian@uma.ac.ir

Mohamadhasan Yazdani
yazdani.m51@gmail.com

Behrouz Sobhani
sobhani@uma.ac.ir

Ata Ghaffari Gilandeh
a_ghafarigilandeh@uma.ac.ir

[1] Geography and Urban and Rural Planning, Faculty of Literature and Humanities, University of Mohaghegh Ardabili, Ardabil, Iran

[2] Physical Geography, Climatology, Faculty of Literature and Humanities, University of Mohaghegh Ardabili, Ardabil, Iran

Published online: 22 June 2020

most common climate phenomena in arid and semi-arid regions of the world and is considered as one of the most important environmental problems in these areas. The consequences of this include social and economic problems, disruption of transportation systems and, in general, environmental crises (Azizi et al. 2011; Christos. 2018). The phenomenon of dust is one of the most important environmental challenges in the region of the Middle East and Iran in recent years. Today, this phenomenon has become one of the main problems in arid and semi-arid regions, which has adverse social, economic and environmental impacts (Fallah et al. 2014; Lilit et al. 2019). The dust storms are one of the environmental hazards in the arid and semi-arid regions of the world. It is an environmental event of climate hazards that causes or exacerbates cardiovascular diseases, respiratory diseases and many allergies in the human body (Naserpour et al. 2015). The dust phenomenon is a complex process that affects Earth-atmosphere interactions and is mainly caused by high-speed winds in arid lands and dry air conditions and often includes arid and semi-arid regions (Ataei et al. 2015). The dust storms are major atmospheric phenomena that have significant effects on the environment, health and social and economic activities due to the entry of dust particles into the atmosphere (Babaei et al. 2016). Dust is always considered as one of the most important environmental hazards and has adverse environmental consequences and it is one of the problems that have been spreading over the last few years due to human interferences and irrational use of natural resources and its degradation (Gandomkar et al. 2017). Other researchers on dust have been investigated, including the following: Karimi and Shokouhi (2011); Shamsipour and Safarrad (2012); Khoshakhlagh et al. (2013); Arnas et al. (2017); Cantarella and Luca (2005); Co and Boosarawongse (2007); Cuevas et al. (2017); Rafał et al. (2016); Monika et al. (2016); Eslam et al. (2017); Niu and Pinker (2015); Dagsson-Waldhauserova et al. (2014); Painter et al. (2012); Meinander et al. (2014); Aher et al. (2014); Bilal et al. (2014); Castelli et al. (2014); Ma and Pinker (2012); Safarianzengir et al. (2019).

Naserpour et al. (2015) investigated the source identification of the dust storms in the southwest of Iran using satellite imagery and aerial maps and concluded that the Sudan low-pressure system brings hot and dry winds polluted with Saudi Arabia dust into our region. Hajbarpour et al. (2015) studied the synoptic and statistical data on the dust phenomenon in Ardabil. They found that the phenomenon of dust has a rising trend and its most frequent occurrence has often occurred at noon hours. Broomandi and Bakhtiarpour (2017) investigated the source identification of dust particles using numerical modelling in Masjed Soleiman and concluded that the main source of dust storms is in Masjed Soleiman. Babaei et al. (2016) investigated the analysis and identification of the synoptic patterns of dust storms and concluded that the mechanisms created dust in the cold season effect on patterns of atmospheric circulation and systems in the Middle East due to the greater diversity. Bagheri and Hosseini (2016) investigated the synoptic analysis of dust in 52 southern cities of Iran and concluded that the formation of a low-altitude mid-tropospheric system on the Saudi Arabia and Iraq was the main cause of the formation of the dust mass. Amarloo et al. (2017) investigated dust particles and its effect on air quality and concluded that the percentage rates of pollutants with a clean, healthy and unhealthy criterion for sensitive, unhealthy, very unhealthy and dangerous groups were 10, 42, 34, 11, 5.2 and 5%, respectively during a year. Sahraei et al. (2017) tracked the dust storms and found that the origin of these storms was the central and northern regions of Iraq and Syria. Gandomkar et al. (2017) investigated the relationship between the temperature series and the days with dust in Hamadan Province and found that the temperature series have been increasing. Arnas et al. (2017) investigated the characteristics and source of large dust particles produced in Alcatorc and found that dust particles such as globes and compresses form the first class and the second class are the dust particles that mainly form due to material coatings. Dansie et al. (2017) measured the characteristics of wind dust and the ability to examine the oceans. They found that dust has significant amounts of portable material than the dust of the main Gulf of South Africa's lake. Sahu et al. (2017) investigated the phenol absorption of the artificial product with active particles and concluded that organic pollutants had a negative effect on the neighbouring environment.

Jixia et al. (2017) investigated the link between biomedical engineering and forestry and dust in Mongolia and concluded that the wind had a strong propaganda effect on dust, while forestry ecosystem engineering and rainfall had an inhibitory effect. Zielhofer et al. (2017) investigated thousands of annual fluctuations in the supply of Syria's dust by reducing drought in Africa and found that increasing the enrichment of dust in the north of the desert on the western shores of the Caspian Sea in the northwestern Mediterranean of Africa. Shoji et al. (2017) studied the simulation of impurity transport in the peripheral plasma due to the release of dust in a long pulse drain on a large cylinder and concluded that plasma is more effective on the release of iron from the heli koks coil and can create carbon dust from the area. Liu et al. (2017) have studied the slope of dust charge under the conditions of the Tokamak plaque. They concluded that the dust particles obtain − 3 in relatively low plasma temperatures (< EV10) and a plasma density of less than 1019 m. Zalesna et al. (2017) studied the dust from JET with the ITER wall, such as the composition and the internal structure. They found that the comprehensive features of a wide range of high-resolution microscopes, including a concentrated ion beam, have led to identifying several particle classes. Willame et al. (2017) investigated the recovery of cloud, dust and ozone in the Martian atmosphere using SPICAM/UV and concluded that

the results of ozone are affected by clouds. Wang et al. (2017) investigated the significant effects of heterogeneous reactions on the chemical composition and mode of dust mixing and concluded that heterogeneous reactions were the main mechanism for producing nitrate and sulphate in dust particles. Aromatic nitrate and ammonium sulphate reduce due to the absorption of acid gas by dust particles. Nabavi et al. (2017) investigated the sensitivity of the predictions of WRF-CHEM to the characteristics of the function of the source of dust in West Asia and found that increasing the mean Spearman correlation between prediction and observations predict the aerosol optical factor by 12 to 16% then run control using standard source functions.

We obtained enough information for the implementation of this research according to the studies carried out. The phenomenon of dust, especially in the western strip of Iran, has always been associated with many problems for residents of these areas. This phenomenon is affected by atmospheric conditions, which cause irreparable damage and respiratory problems every year. In addition, the phenomenon reduces air quality. Therefore, it is necessary to pay attention to the issue of dust. The purpose of this research is to evaluate and predict the hazards of dust using the hybrid artificial neural network developed based on the TOPSIS and simple additive weighting (SAW) multi-criteria decision-making models.

Materials and methods

Area of research

The western region of Iran includes 4 provinces: Ilam, Kermanshah, Khuzestan and Lorestan. The southwestern part of Iran is geographically included regions with their particular climate which suffers a lot of natural damages each year. The studied area and the geographic characteristics of the 14 stations studied are presented in (Fig. 1).

Research method

The 29-year dust data (1990–2018) were used to analyse and predict the dust in the western strip of Iran. Panel data-hybrid artificial neural network and adaptive neuro-fuzzy inference system (ANFIS) were used for error detecting and predicting, then the new models of TOPSIS and SAW multi-criteria decision-making (MCDM) were used to identify areas more exposed to the dust phenomenon.

Experimental pattern

A two-way error component model is used based on the panel data framework in Eq. (1).

$$L_nP_{it} = \mu_i + \lambda_t + \beta_i L_n \mathrm{ER}_{it} + v_{it} \tag{1}$$

where LnPit is logarithm the value of each unit of the amount of dust (14 stations studied). The unobservable effects are divided into two groups of effects of the frequency of dust and time effects (Gujarati 2003; Woldridge 2006).

Prediction with panel data model

At first, the forecast is described based on a one-way error component model. The best linear predictor for $T+S$, y_i without bias for the prediction of the next period S for the section ith is as in Eq. (2) (Baltagi 2005; Sobhani et al. 2018).

$$\widehat{y}_{i,T+S} = Z'_{i,T+S}\delta_{GLS} + w'\Omega\widehat{u}_{GLS} \quad \text{for} \quad s \geq 1 \tag{2}$$

where Y is a vector with dimensions $X, Z = [l\ NT, X]$, $NT \times 1; 1\ NT, NT \times K$ is a unit vector with a dimension of $\Omega = \delta = (\alpha, \beta), NT\widehat{u}_{GLS} = -Z\widehat{\delta}_{GLS}$ and $(w = \mathrm{E}\ u_{i,\ T} + S^u)$ are a variance-covariance matrix, respectively, for period $T+S$ (Eq. (3)).

$$u_{i,T+S} = \mu + v_{i,T+S} \tag{3}$$

And $w = \delta_u^2(l_i \otimes l_T)$, in which L_i is the column it from the unit matrix and it is I_n. For example, I_i is a vector of 1 for the observation and 0 for other observations. Therefore, we will have Eq. (4):

$$w'\Omega^{-1} = \sigma_\mu^2\left(l_i' \otimes i_T'\right)\left[\frac{1}{\sigma_1^2}P + \frac{1}{\sigma_v^2}Q\right] = \frac{\sigma_\mu^2}{\sigma_1^2}\left(l_i' \otimes i_T'\right) \tag{4}$$

given that $l_i' \otimes l_i' P = \left(l_i' \otimes l_T'\right)$ and $\left(l_i' \otimes l_T'\right)Q = 0$. According to Eq. (4), $w'\Omega^{-1}\widehat{u}_{\mathrm{GLS}}$ is converted to $\left(\left(T\sigma_\mu^2/T\sigma_I^2\right)\widehat{u}_{i,GLS}\right)$ that $\widehat{u}_{i.GLS} = \sum_{i=1}^{T}\widehat{u}_{it,GLS}/T$. Therefore, the best predictor corrects the predictions without bias through the ratio of mean residuals for $T+S$, y_i in Eq. (4). In the two-way error component model for each $T+S$ period, we will have Eqs. (5) and (6).

$$u_{i,T+S} = \mu_i + \lambda_{T+S} + v_{i,T+S} \tag{5}$$

$$\begin{aligned} i = j \quad &\text{for} \quad E\left(u_{i,T+S}u_{jt}\right) = \sigma_\mu^2 \\ i \neq j \quad &\text{for} \quad E\left(u_{i,T+S}u_{jt}\right) = 0 \end{aligned} \tag{6}$$

Therefore, $w = E\left(u_{i,T} + s^u\right) = \sigma_u^2(l_l l_T)$ is consistent for the best predictor without linear bias in Eq. (2) and I_i is a column with of the unit matrix with $N \times N$ dimensions. So, Eq. (7) is as follows:

$$w'\Omega^{-1} = \sigma_\mu^2\left(l_i' \otimes i_T^i\right)\left[\sum_{i=l}^{4}\frac{1}{\lambda_i}Q_i\right] \tag{7}$$

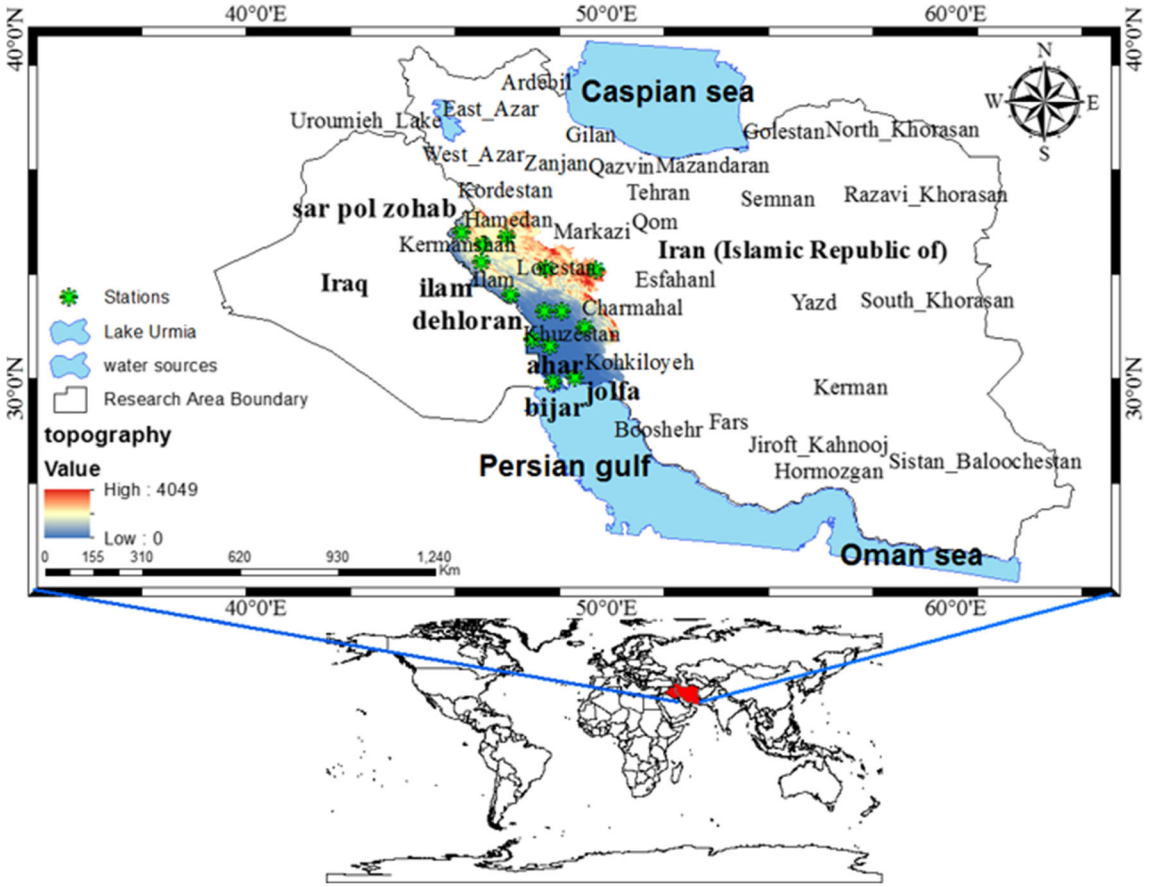

Fig. 1 Region and the stations under research in the world

According to Eqs. (8) and (9):

$$\left(l_i' \otimes i_T'\right) Q_1 = 0 \quad \left(l_i' \otimes i_T'\right) Q_2 = \left(l_i' \otimes i_T'\right) - i_{NT}'/N \tag{8}$$

$$\left(l_i' \otimes i_T'\right) Q_3 = 0 \quad \left(l_i' \otimes i_T'\right) Q_4 = i_{NT}'/N \tag{9}$$

Equation (10) is obtained:

$$w'\Omega^{-1} = \frac{\sigma_\mu^2}{\lambda_2}\left[\left(l_i' \otimes i_T'\right) - i_{NT}/N\right] + \frac{\sigma_\mu^2}{\lambda_4}\left(i_{NT}/N\right) \tag{10}$$

Therefore, $w'\Omega^{-1}\widehat{u}_{\mathrm{GLS}}$ (That $\widehat{u}_{\mathrm{GLS}} = y - Z\sigma_{\mathrm{GLS}}$) is as in Eq. (11):

$$\frac{T\sigma_\mu^2}{\left(T\sigma_\mu^2 + \sigma_v^2\right)}\left(\overline{\widehat{u}}_{i0,\mathrm{GLS}} - \overline{\widehat{u}}_{00,\mathrm{GLS}}\right) + \frac{T\sigma_\mu^2}{\left(T\sigma_\mu^2 + N\sigma_\lambda^2 + \sigma_v^2\right)}\overline{\widehat{u}}_{00,\mathrm{GLS}} \tag{11}$$

where $\overline{\widehat{u}}_{i,\mathrm{GLS}} = \sum_{i=I}^{T}\overline{\widehat{u}}_{it,\mathrm{GLS}}/T$ and $\overline{\widehat{u}}_{\ldots,\mathrm{GLS}} = \sum_i\sum_t \widehat{u}_{it,\mathrm{GLS}}/NT$. Therefore, the best predictor without linear bias for $T+S$, y_i is correct by using mean residuals for the two-way error component model as in Eq. (12):

$$\widehat{y}_{i,T+S} = Z_{i,T+S}'\widehat{\delta}_{\mathrm{GLS}} + \left(\frac{T\sigma_\mu^2}{T\sigma_\mu^2 + \sigma_v^2}\right)\overline{\widehat{u}}_{i,\mathrm{GLS}} \tag{12}$$

Prediction with panel data-hybrid artificial neural network model

An artificial neural network is a parallel distributed processing model that consists of several main processing functions or units. The activator functions used in the neural network often are linear, sigmoid and hyperbolic. Specifying an artificial neural network is based on observations, and given the finite points, many functions can be found to fit well (Co and Boosarawongse 2007; Sobhani et al. 2019a).

Introducing criteria for comparing and evaluating precision in prediction methods

The criteria such as mean square error (MES), root mean square error (RMSE), mean absolute error (MAE) and mean absolute percentage error (MAPE) are used to compare and evaluate different prediction methods (Table 1). The values i_y, y_i and n represent the predicted values, actual values and the number of data, respectively (Tohidi et al. 2015; Sobhani et al. 2019b).

Adaptive neuro-fuzzy inference systems

The fuzzy system is a system based on the "condition-result" logical rules that it depicts the space of input variables on the space of the output variables by using the concept of linguistic variables and fuzzy decision-making process. The combination of fuzzy systems based on logical rules, and artificial neural network methods that can extract the knowledge from numerical data, has led to the introduction of an adaptive neural inference system. A Sogno fuzzy system with two inputs, one output and two rules and adaptive neuro-fuzzy inference system (ANFIS) is presented in (Fig. 2). This system has two inputs x and y and one output f. The structure of ANFIS consists of five layers as follows: if the output of each layer is Q_i^1 (i and it the node of layer j) (Ahmadzadeh et al. 2010). In the end, the error rates of the resulting models were compared and the function that produces the lowest error rate at the lowest training time (Fig. 2) will be selected as a membership function. Generally, entering raw data reduces the speed and precision of the networks.

Therefore, net inputs should be placed in the range of the sigmoid function (between 0 and 1) to prevent the early saturation of the neurons and to equalize the value of the data for the network. This prevents too much underweight and reduces the early saturation of the neurons (Kenarkoohi et al. 2010; Sobhani & Safarianzengir 2019).

Proximity to ideal mode (TOPSIS)

Hwang and Yoon proposed TOPSIS in 1981. In this method, m alternatives (A1, A2... Am) were evaluated with the n indices (C1, C2, ..., Cn). Solving this problem with this method involves the following steps (Makvandi et al. 2012; Nazmfar and Alibakhshi 2014):

1. Un-scaling of decision matrix using norm un-scaling (Eq. (13)):

$$r_{ij} = \frac{f_{ij}}{\sqrt{\sum_{j=1}^{j} f_{ij}^2}} \qquad j = 1, \ldots, J \qquad i = 1, \ldots, n \tag{13}$$

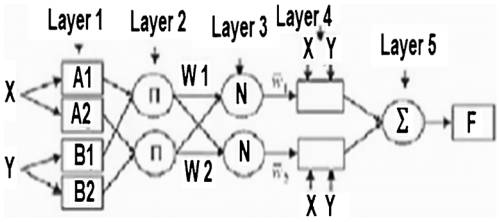

Fig. 2 Sogno fuzzy system with triangular membership function and its equivalent ANFIS system (Kisi and Ozturk 2007)

2. Formation of the weighted unscaled matrix (V_{ij}) by multiplying the unscaled matrix (r_{ij}) in weight diagonal matrix (Eq. (14))

$$v_{ij} = w_i \times r_{ij} \qquad j = 1, \ldots, J \qquad i = 1, \ldots, n \tag{14}$$

where W_i is the weight of the ith index, and the total weight of indices equals 1.

3. Determination of positive (A^*) and negative (A^-) The ideal solution is as shown in Eqs. (15) and (16):

$$A^* = \{v_1^*, \ldots, v_n^*\} = \{(\max_j v_{ij} | i \in I'), (\min_j v_{ij} | i \in I'')\} \tag{15}$$

$$A^- = \{v_1^-, \ldots, v_n^-\} = \{(\min_j v_{ij} | i \in I'), (\max_j v_{ij} | i \in I'')\} \tag{16}$$

4. Determination of distance of each alternative to the positive and negative ideals.

The distance of each alternative to the positive ideal (D_j^*) is as shown in Eq. (17):

$$D_j^* = \sqrt{\sum_{i=1}^{n} \left(v_{ij} - v_j^*\right)^2} \quad , \quad j = 1, \ldots, J \tag{17}$$

Table 1 Criteria for comparing and evaluating precision in prediction. Reference: Tohidi et al. (2015)

Criteria	Equations
Mean Square error (MSE)	$\mathrm{MSE} = \frac{1}{n} \sum_{i=1}^{n} (y_i - \widehat{y}_i)^2$
Root mean square error (RMSE)	$\mathrm{RMSE} = \sqrt{\frac{1}{n} \sum_{i=1}^{n} (y_i - \widehat{y}_i)^2}$
Mean absolute error (MAE)	$\mathrm{MAE} = \frac{1}{n} \sum_{i=1}^{n} \lvert y_i - \widehat{y}_i \rvert$
Mean absolute percentage error (MAPE)	$\mathrm{MAPE} = \frac{1}{n} \sum_{i=1}^{n} \left\lvert \frac{y_i - \widehat{y}_i}{y_i} \right\rvert \times 100$

The distance of each alternative to the negative ideal (D_j^*) is as shown in Eq. (18):

$$D_j^- = \sqrt{\sum_{i=1}^{n}\left(v_{ij}-v_j^-\right)^2} \quad , \quad j = 1, \ldots, J \tag{18}$$

5. Determination of relative proximity of each alternative to the ideal solution (Eq. (19)):

$$C_j^* = \frac{D_j^-}{D_j^* + D_j^-} \quad , \quad j = 1, \ldots, J \tag{19}$$

6. Ranking alternatives based on relative proximity $\left(C_j^*\right)$, the alternative greater is better.

Simple additive weighting method

1. It is simple to use the SAW method to select the best option if there are a criterion and *m* alternative in multi-criteria decision-making.
2. Formation decision matrix: The decision matrix of this method consists of a table with the columns as criteria or sub-criteria, and the rows as alternatives (stations)
3. Un-scaling of the decision matrix:

We divide each of the numbers of the column into the largest number, if the criterion is positive (Eq. (20)), and if the criterion is negative (Eq. (21)), the minimum of the column is divided into each number.

$$r_{ij} = \frac{x_{ij}}{x_j \max} \tag{20}$$

$$\frac{r_{ij} = x_j \min}{x_{ij}} \tag{21}$$

4. Formation of a weighted matrix: The weighted matrix is obtained using other methods (Eq. (22))

$$W_i = \sum_{j=1}^{n} w_j \times r_{ij} \tag{22}$$

5. Choosing the best alternative: The score for each alternative is computed by adding the weight matrix rows and are ranked according to Eq. (23).

Table 2 Mean training and validation error of stations in the north of the Persian Gulf, Iran

Station	Mean validation error	Mean training error
Bostan	15.43	01.019
Safi Abad	5.12	0.01
Abadan	1.12	03.00
Dezful	6.1	06.07
Masjed Soleiman	2	0.09
Bandar-e Mahshahr	1.33	09.010
Ahwaz	9.66	08.014
Kermanshah	10.78	06.07
Eslamabad-e Gharb	12.98	01.019
Sarpol-e Zahab	1.11	02.08
Ilam	8.63	011.016
Dehloran	13.09	014.010
Khorramabad	1.25	04.014
Aligudarz	4.69	019.02

$$A^* = \left\{ A_i | \max \frac{\sum_{j=1}^{n} w_j r_{ij}}{\sum w_j} \right\} \tag{23}$$

Results and discussion

The purpose of this study was to investigate dust in the western strip of Iran. So, a new model in climatology, the panel data-artificial neural network hybrid model, was used. The new and developed models of TOPSIS and SAW multi-criteria decision-making were used to prioritize more dust-prone areas.

Validation and initial validation for prediction

Regarding the modelling based on ANFIS for forecasting station dust, the lowest mean training error and the mean validation error was obtained 0.01 for Safiabad station and 1.11% for Sarpol Zahab station. The highest mean training error and the mean validation error was related to Aligudarz station (019.02) and Bostan station (15.43%), respectively. The training and validation errors of other stations are presented in (Table 2).

Fig. 3 Trend and time series of observed and predicted years of dust: **a** 5 stations of Bostan, Safiabad, Abadan, Dezful and Masjed Soleiman; **b** 5 stations of Bandar Mahshahr, Ahvaz, Eslamabad Gharb, Sarpol Zahab and Kermanshah; **c** 4 stations of Dehloran, Ilam, Aligudarz and Khorramabad; in the north of the Persian Gulf, Iran

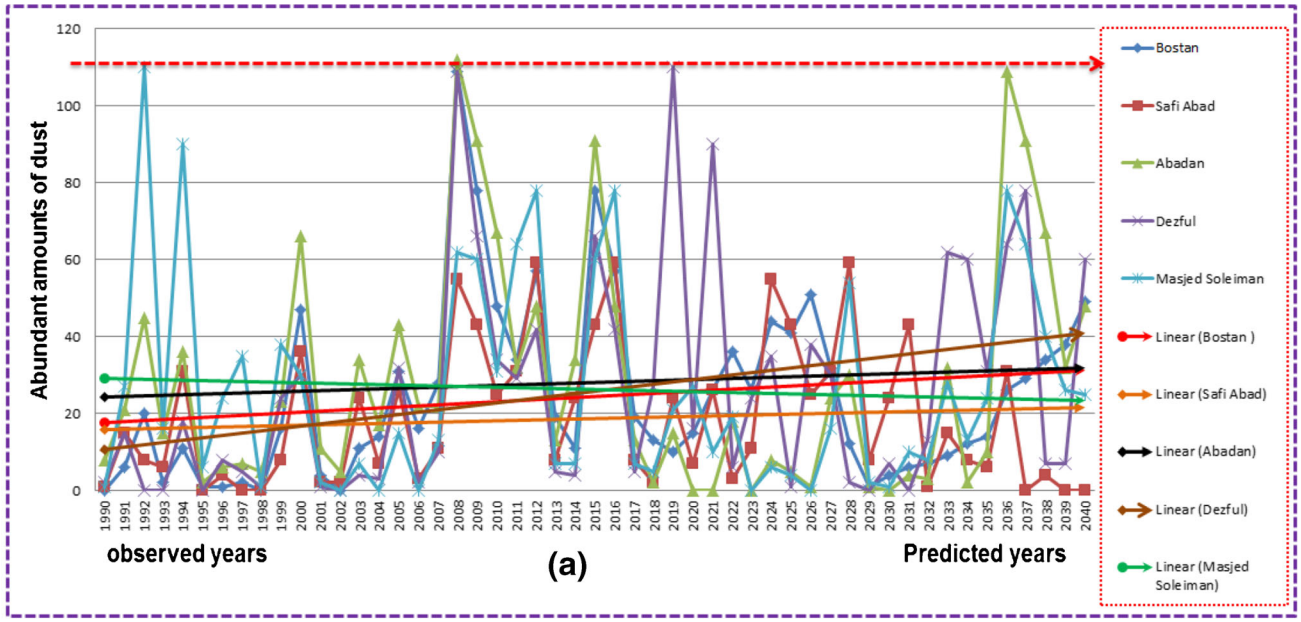
Abundant amounts of dust
observed years
Predicted years
(a)
Bostan
Safi Abad
Abadan
Dezful
Masjed Soleiman
Linear (Bostan)
Linear (Safi Abad)
Linear (Abadan)
Linear (Dezful)
Linear (Masjed Soleiman)

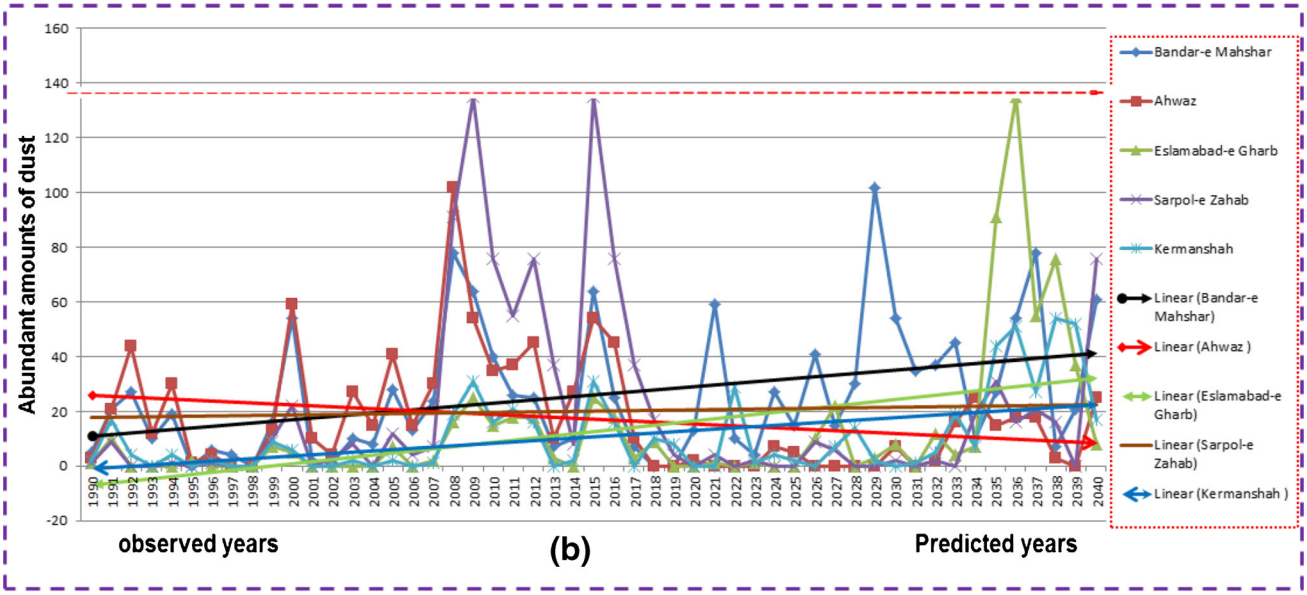
Abundant amounts of dust
observed years
Predicted years
(b)
Bandar-e Mahshar
Ahwaz
Eslamabad-e Gharb
Sarpol-e Zahab
Kermanshah
Linear (Bandar-e Mahshar)
Linear (Ahwaz)
Linear (Eslamabad-e Gharb)
Linear (Sarpol-e Zahab)
Linear (Kermanshah)

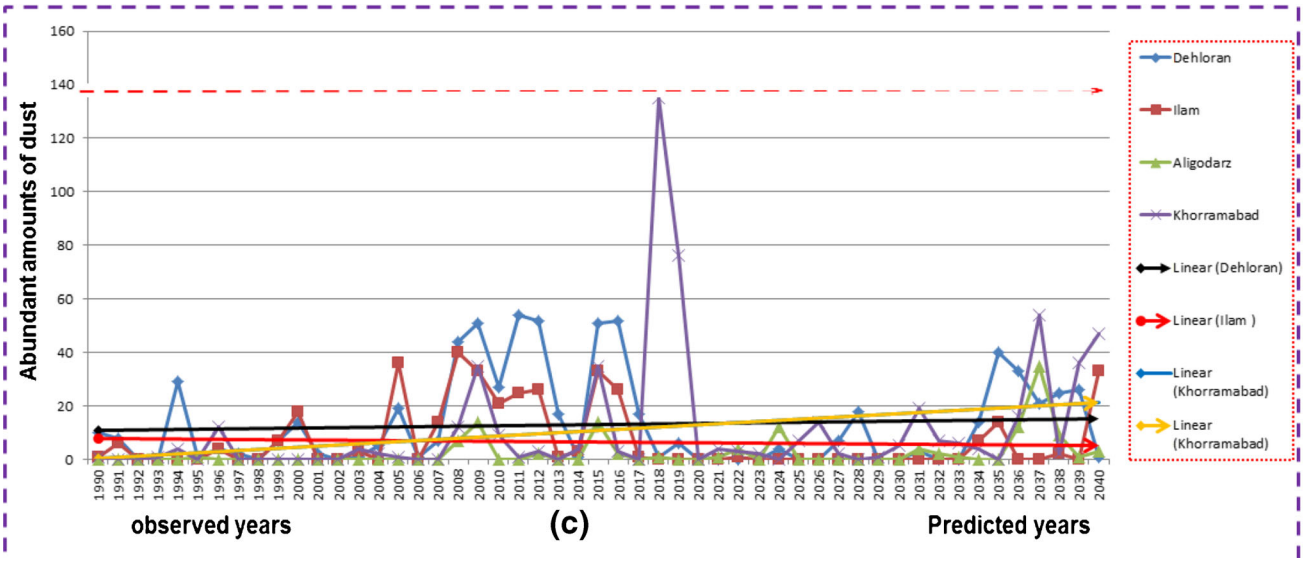
Abundant amounts of dust
observed years
Predicted years
(c)
Dehloran
Ilam
Aligodarz
Khorramabad
Linear (Dehloran)
Linear (Ilam)
Linear (Khorramabad)
Linear (Khorramabad)

Predict the frequency of dust in the future

According to the error detection and validation, it can be predicted more confidently. So, the panel data-artificial neural network hybrid model and panel data model were used. Dezful station with 110.11% in 2019, Abadan station with 109.12% in 2036, Bandar Mahshahr station with 102.04% in 2029 (Fig. 3a), Eslamabad Gharb station with 135.19% (Fig. 3b) and Khorramabad station with 54.87% of the frequency of the dust (Fig. 3c) showed an increasing trend.

Evaluation of the function of the predictive models after prediction

After predicting the stations related to the regression model of the two-way error component and panel data-artificial neural network hybrid model, the function of the predictions of these two models was evaluated based on precision criteria. The results of the model evaluations are separately presented for each of the stations in (Table 3).

Zoning frequency of the dust

According to the data obtained from the predictions, the mean frequency of dust at 14 stations was zoned. The stations of Sarpol Zahab, Masjed Soleiman and Abadan showed the maximum dust frequency (29.21, 31.447 and 33.46, respectively) and the minimum dust frequency was observed at the two stations of Aligudarz and Khorramabad (1.428 and 2.428, respectively) (Fig. 4a). Considering the maximum dust frequency, the highest dust was related to Sarpol Zahab and Abadan stations (128.917 and 120.709, respectively) and the lowest dust frequency belonged to the stations of Aligudarz, Eslamabad Gharb and Khorramabad (14.05, 20.023 and 28.29, respectively) (Fig. 4b).

Table 3 Comparing and evaluating prediction precision for each station in the north of the Persian Gulf, Iran

Stations	Prediction method	Precision criteria			
		MSE	RMSE	MAE	MAPE
Bostan	Panel data model	0.0071	0.0632	0.0516	0.4159
	Panel data-artificial neural network hybrid model	0.0003	0.0135	0.0215	0.2113
Safiabad	Panel data model	0.0051	0.0036	0.0951	0.0009
	Panel data-artificial neural network hybrid model	0.0214	0.0012	0.0006	0.0014
Abadan	Panel data model	0.0065	0.0054	0.0852	0.0085
	Panel data-artificial neural network hybrid model	0.0615	0.0587	0.0456	0.0025
Dezful	Panel data model	0.0361	0.0031	0.0321	0.0009
	Panel data-artificial neural network hybrid model	0.0069	0.0149	0.0951	0.0006
Masjed Soleiman	Panel data model	0.0478	0.0011	0.0007	0.0154
	Panel data-artificial neural network hybrid model	0.0698	0.0198	0.0147	0.0852
Bandar-e Mahshahr	Panel data model	0.0014	0.0033	0.0752	0.0845
	Panel data-artificial neural network hybrid model	0.0019	0.0098	0.0159	0.0698
Ahvaz	Panel data model	0.0014	0.00001	0.0456	0.0257
	Panel data-artificial neural network hybrid model	0.0009	0.0014	0.0001	0.0632
Kermanshah	Panel data model	0.0147	0.0362	0.0003	0.0005
	Panel data-artificial neural network hybrid model	0.0385	0.0987	0.0741	0.0124
Eslamabad Gharb	Panel data model	0.0415	0.0654	0.0145	0.0397
	Panel data-artificial neural network hybrid model	0.0063	0.0005	0.0321	0.0125
Sarpol Zahab	Panel data model	0.0785	0.0222	0.0008	0.0129
	Panel data-artificial neural network hybrid model	0.0965	0.0111	0.0032	0.0012
Ilam	Panel data model	0.0004	0.0569	0.0021	0.0317
	Panel data-artificial neural network hybrid model	0.0098	0.0007	0.0059	0.0123
Dehloran	Panel data model	0.0021	0.0258	0.0014	0.0036
	Panel data-artificial neural network hybrid model	0.0369	0.0987	0.0029	0.0198
Khorramabad	Panel data model	0.0011	0.0741	0.0018	0.0013
	Panel data-artificial neural network hybrid model	0.0015	0.0963	0.0087	0.0843
Aligudarz	Panel data model	0.0177	0.0357	0.0852	0.0069
	Panel data-artificial neural network hybrid model	0.0333	0.0753	0.0125	0.0852

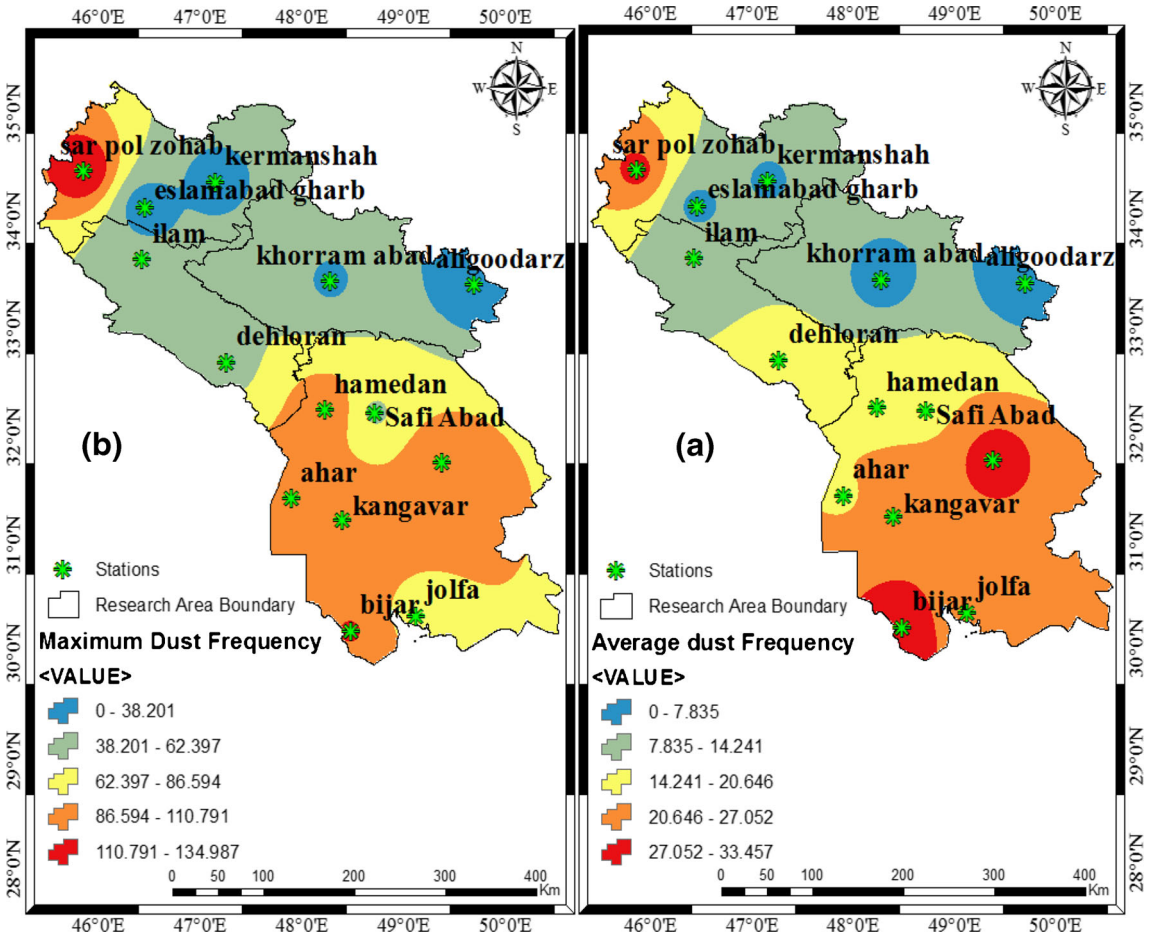

Fig. 4 Dust frequency obtained from predictions in the north of the Persian Gulf, Iran. **a** Average dust frequency. **b** Maximum dust frequency

Table 4 Priority dust-prone stations based on SAW and TOPSIS models in the north of the Persian Gulf, Iran

Row	Stations	TOPSIS Model		SAW Model	
		Rank	Score	Rank	Score
1	Bostan	4	0.4987	0.5944	6
2	Safiabad	3	0.5222	0.5753	8
3	Abadan	10	0.1721	1	1
4	Dezful	5	0.4986	0.5944	7
5	Masjed Soleiman	9	0.0893	0.9273	2
6	Bandar Mahshahr	6	0.4502	0.6383	5
7	Ahvaz	7	0.2481	0.7982	4
8	Eslamabad Gharb	1	1	0.1867	10
9	Sarpol Zahab	8	0.1746	0.858	3
10	Kermanshah	2	0.9659	0.2142	9
11	Dehloran	14	0.11	0.1632	11
12	Ilam	13	0.1407	0.1232	12
13	Aligudarz	11	0.1732	0.12	14
14	Khorramabad	12	0.1623	0.11	13

Prioritizing the dust-prone areas for stations based on TOPSIS and SAW models in the western strip of Iran

After validation and error detection and prediction of the frequency of dust in stations based on two SAW and TOPSIS models, the frequency of dust was prioritized and then was zoned. The goal of the TOPSIS method, one of the new methods for solving multi-criteria decision-making problems, is to select the best option based on the closest possible answer to the ideal answer.

Therefore, appropriate indicators, statistical methods and multi-criteria decision-making techniques were studied and selected, using the TOPSIS model, to rank the stations studied in terms of the frequency of dust to select the dust-prone areas for the in the next 23 years. The Eslamabad Gharb and Kermanshah stations (0.997 and 0.9659%, respectively) will be more exposed to dust and the Dehloran and Ilam stations with the lowest frequency of the dust (0.11 and 0.1407%, respectively) have the minimum dust frequency (Table 4, Fig. 5a). Based on the SAW model, the stations of Abadan and Masjed Soleiman were more exposed to the dust (0.998 and 0.92, respectively) and the lowest frequency of the dust belonged to the stations of Aligudarz and Khorramabad (Table 4, Fig. 5b).

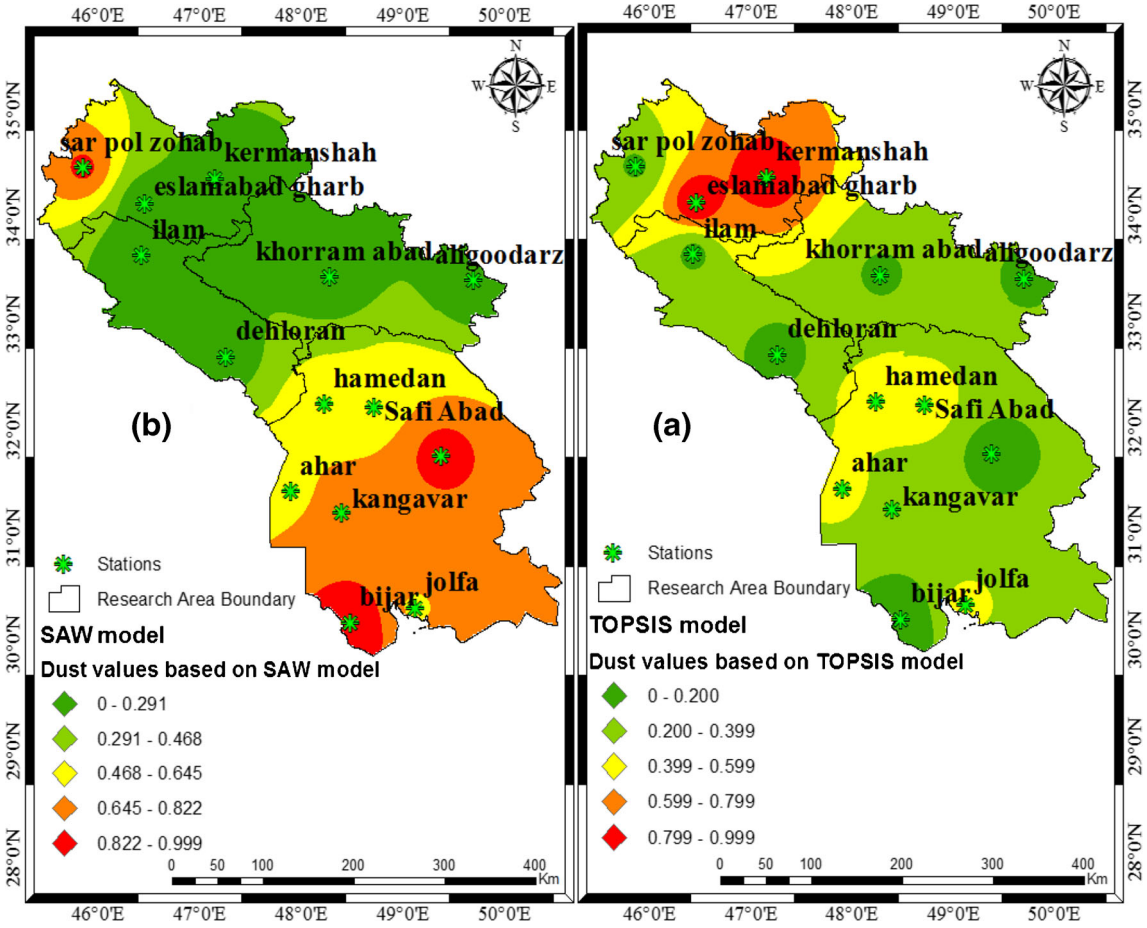

Fig. 5 The final map of dust-prone areas in the north of the Persian Gulf, Iran. **a** TOPSIS model. **b** SAW model

Comparison of research results with findings of other researchers

In this research, we studied analysis, monitoring and simulation of dust hazard phenomenon in the northern Persian Gulf, Iran, Middle East. This method has been used in many types of research and it has been considered as a suitable method for monitoring, analysis and comparison, for example:

Competing droughts affect dust delivery to Sierra Nevada (Aarons et al. 2019)
Depositional characteristics of ^{7}Be and ^{210}Pb in Kuwaiti dust (Aba et al. 2016)
The role of dominant perennial native plant species in controlling the mobile sand encroachment and fallen dust problem in Kuwait (Ahmed et al. 2016)
Health impact assessment associated with exposure to PM10 and dust storms in Kuwait (Al-Hemoud et al. 2018)
Effects of atmospheric dust deposition on solar PV energy production in a desert environment (Christos et al. 2018)
Meteorological catalysts of dust events and particle source dynamics of affected soils during the 1930s Dust Bowl drought (Kasey et al. 2019)
Contamination levels and human health risk assessment of mercury in dust and soils of the urban environment (Lilit et al. 2019)
Experimental study on dust suppression at transshipment point based on the theory of induced airflow dust production (Xinghua et al. 2019)

However, models in the present study were useful in modelling, monitoring and predicting the dust phenomenon in the north of the Persian Gulf, Iran.

Conclusion

The dust phenomenon annually causes irreparable damages to various parts of the life of the living organisms and the environment. Due to the importance of this issue, researchers have sought to address this issue in the vast region of Iran with a lot of stations. In this study, the hazardous phenomena of dust in the western strip of Iran were investigated in Khuzestan, Ilam,

Lorestan and Kermanshah Provinces using panel data and hybrid neural network models. The result shows that the phenomenon of dust is increasing in most of the studied stations. The dust data was used to predict the two models of the adaptive neural network (ANFIS) and the hybrid neural network and concluded that the power of the hybrid neural network was more than the adaptive neural network (ANFIS). According to the comparison and evaluation carried out for prediction, the highest mean frequency of the dust was observed at three stations of Sarpol Zahab, Masjed Soleiman and Abadan (29.21, 31.447 and 33.46%, respectively).

According to the model of data panel and hybrid neural network, evaluation and comparison of the models showed that the lowest MSE in the hybrid model was 00019 at the station of Bandar Mahshahr and in the panel data model, 0.0004 was obtained at Ilam station. The lowest RMSE was shown in the hybrid model at Eslamabad Gharb station (0.00005) and in the data panel model at Ahwaz station (0.0001). The lowest MAE was obtained in the hybrid model at Ahwaz station)0.00001 (and in the data panel model was at Sarpol Zahab station (0.0008) and the lowest MAPE was shown in the hybrid model at Ahwaz station (0.00006) and in the data panel model at Sarpol Zahab station (0.0005). Finally, according to the TOPSIS model, the stations of Eslamabad Gharb and Kermanshah were more exposed to the dust in the future (0.997 and 0.9659, respectively). Based on the SAW model, the stations of Abadan and Masjed Soleiman will have the maximum probability of dust occurrence (0.998 and 0.92, respectively) in the future. Considering the results for reducing the hazards of dust in the studied area, the relevant organizations should make serious decisions on this subject.

Acknowledgments The authors would like to thank the I.R. of Iran Meteorological Organization (IRIMO) for providing the meteorological data for this study. We also would like to thank Prof. Majid Rezaei Banafsheh for the support in writing. We also acknowledge the support from Mohaghegh Ardabili University.

Data availability Upon the acceptance of the article, the data used in this research will be released.

Compliance with ethical standards

Conflict of interests The author declares that they have no conflict of interest.

References

Aarons SM, Arvin LJ, Aciego SM, Riebe CS, Johnson KR, Blakowski MA, MKoornneef J, Hart SC, Barnes ME, Dove N, Botthoff JK, Maltz M, Aronson EL (2019) Competing droughts affect dust delivery to Sierra Nevada. Aeolian Res 41:100545. https://doi.org/10.1016/j.aeolia.2019.100545

Aba A, Al-Dousari M, Ismaeel A (2016) Depositional characteristics of ^{7}Be and ^{210}Pb in Kuwaiti dust. J Radioanal Nucl Chem 4:453–468. https://doi.org/10.1007/s10967-015-4129-y

Aher GR, Pawar GV, Gupta P, Devara PCS (2014) Effect of major dust storm on optical, physical, and radiative properties of aerosols over coastal and urban environments in Western India. Int J Remote Sens 35:871–903. https://doi.org/10.1080/01431161.2013.873153

Ahmadzadeh G, Mirlotfi SM, Mohammadi K (2010) Comparison of Artificial Intelligence Systems (ANN & ANFIS) for reference evapotranspiration estimation in the extreme arid regions of Iran. J Water Soil 24:679–689 [In Persian]

Ahmed M, Al-Dousari N, Al-Dousari A (2016) The role of dominant perennial native plant species in controlling the mobile sand encroachment and fallen dust problem in Kuwait. Arab J Geosci ProScience 1:273–277. https://doi.org/10.1007/s12517-015-2216-6

Al-Hemoud A, Al-Dousari A, Ahmad AS, Al-Khayat A, Behbehani W, Malak M (2018) Health impact assessment associated with exposure to PM10 and dust storms in Kuwait. Atmosphere 9:6. https://doi.org/10.3390/atmos9010006

Amarloo J, Javid H, Shekarian R, Rezaei F, Vahdani A (2017) Dust particles and their impact on air quality. The Fourth International Conference on Environmental Planning and Management 41–36. [In Persian]

Arnas C, Lrby J, Celli S, Detemmerman G, Addab Y, Couedel L, Grisolia C, Lin Y, Martin C, Pardanaud C, Pierson S (2017) Characterization and origin of large size dust particles produced in the alcator C_ mod tokamak. Nuchear Mater Energy 11:12–19

Ataei SH, Mohammadzadeh A, Akbar AA (2015) Using decision tree method for dust detection from MODIS satellite image. J Geomatics Sci Technol 4:151–160 [In Persian]

Azizi GH, Miri M, Nabavi SO (2011) Detection of dust in the midwest of Iran. J Arid Regions Geogr Stud 2:103–118 [In Persian]

Babaei PH, Safarrad T, Karimi M (2016) Analysis and identification of synoptic patterns of dust storms in west of Iran. J Geogr Environ Hazards 5:119–105 [In Persian]

Bagheri Z, Hosseini S.M (2016) Synoptic analysis of dust in 52 cities of South Iran. First International Conference on Natural Hazards and Environmental Crises in Iran. Solutions to Challenges 29–26. [In Persian]

Baltagi BH (2005) Econometric analysis of panel data, 3rd edn. Wiley, New York

Bilal M, Nichol JE, Chan PW (2014) Validation and accuracy assessment of a simplified aerosol retrieval algorithm (SARA) over Beijing under low and high aerosol loadings and dust storms. Remote Sens Environ 153:50–60. https://doi.org/10.1016/j.rse.2014.07.015

Broomandi P, BakhtiarPour A (2017) Dust source identification using physical-chemical characterization and numerical modeling in Masjed Soleyman. Iran J Health Environ 9:517–526 [In Persian]

Cantarella GE, Luca SDE (2005) Multilayer feedforward networks for transportation mode choice analysis: an analysis and a comparison with random utility models. Transp Res Part C Emerg Technol 13:121–155

Castelli M, Stöckli R, Zardi D, Tetzlaff A, Wagner JE, Belluardo G, Zebisch M, Petitta M (2014) The HelioMont method for assessing solar irradiance over complex terrain: validation and improvements. Remote Sens Environ 152:603–613. https://doi.org/10.1016/j.rse.2014.07.018

Christos F, Benjamin F, Luis A, Mohammed A (2018) Effects of atmospheric dust deposition on solar PV energy production in a desert environment. Sol Energy 164:94–100. https://doi.org/10.1016/j.solener.2018.02.010

Co HC, Boosarawongse R (2007) Forecasting Thailand's rice export: statistical techniques Vs artificial neural networks. Comput Ind Eng 53:610–627

Cuevas E, Gomez-Plelaz AG, Rodriguez S, Terradellas E, Basart S, Garcia RD, Garcia OE, Alonso S (2017) The pulsating nature of large scale Saharan dust transport. Atmos Environ 167:586–602

Dagsson-Waldhauserova P, Arnalds O, Olafsson H (2014) Long-term variability of dust events in Iceland. Atmos Chem Phys Discuss 14:17331–17358. https://doi.org/10.5194/acpd-14-17331-2014

Dansie AP, Wigs GFS, Thomas DSG, Washington R (2017) Measurements of windblown dust characteristics and ocean fertilization potential. Aeolian Res 29:30–41

Dastcherdi J, Mousavi H, Kashki A (2011) A synoptic analysis of Ilam's dust storms. J Geogr Environ Plan 46:34–15

Eslam J, Aliakbar A, Per S (2017) A MODIS-based modeling scheme for the estimation of downward surface shortwave radiation under cloud-free conditions. Arab J Geosci 10:392. https://doi.org/10.1007/s12517-017-3187-6

Fallah M, Vafaeinejad A, Kheirkhah M, Ahmadi F (2014) Monitoring and synoptic analysis of dust. Geogr Inform 91:80–69 [In Persian]

Gandomkar A, Fanaei R, Daneshvar F, Kardan H, Ahadinejad M, Rezaei N (2017) Investigation of temperature series trends and dust days in Hamedan province. Geography 15:293–277 [In Persian]

Gujarati DN (2003) Basic econometrics, 4th edn. McGraw-Hill, New York

Hajbarpour B, Zarei Z, Halimi M, Rostami M (2015) Investigation of changes in height and thickness of boundary layer in dusty conditions of Ahvaz city. Journal of Spatial Analysis of Environmental Hazards 2(8):51–64 [In Persian]

Jixia H, Qibin Z, Jing T, Depeng Y, Quansheng G (2017) Association between forestry ecological engineering and dust weather in Inner Mongolia. Physics and chemistry of the earth, parts A/B/C, in press, corrected proof. available online 2

Karimi AM, Shokouhi K (2011) Interaction between atmospheric circulation and land cover in the mechanism of creation of summertime dust storms in Middle East. Phys Geogr Res 43:112–130 [In Persian]

Kasey B, Mark S, Steven F (2019) Meteorological catalysts of dust events and particle source dynamics of affected soils during the 1930s Dust Bowl drought, Southern High Plains, USA. Anthropocene 27: 100216. https://doi.org/10.1016/j.ancene.2019.100216

Kenarkoohi O, Soleimanjahi H, Fallahi SH, RiahiMadvar H, Meshkat Z (2010) The application of the new intelligent Adaptive Nero Fuzzy Inference System (ANFIS) in prediction of human papilloma virus oncogenic potency. J Arak Univ Med Sci 4:95–105 [In Persian]

Khoshakhlagh F, Najafi MS, Samadi M (2013) An analysis on synoptic patterns of springtime dust occurrence in west Iran. Phys Geogr Res 44:99–124 [In Persian]

Khoshkiysh A, Alijani B, Hejazizadeh Z (2012) Synoptic analysis of dust systems in Lorestan Province. Appl Geosci Res 18:110–191 [In Persian]

Kisi O, Ozturk O (2007) Adaptive neurofuzzy computing technique for evapotranspiration estimation. J Irrig Drain Eng ASCE 4:368–379

Lilit S, Gevorg T, Nairuhi M, Mkhitar K, Gayane M, Armen S (2019) Contamination levels and human health risk assessment of mercury in dust and soils of the urban environment, Vanadzor, Armenia. Atmos Pollut Res 10:808–816. https://doi.org/10.1016/j.apr.2018.12.009

Liu Z, Wang D, Miloshevsky G (2017) Simulation of dust grain charging under tokamak plasma conditions. Nucl Mater Energy 12:530–535

Ma Y, Pinker RT (2012) Modeling shortwave radiative fluxes from satellites. J Geophys Res Atmos 117:D23202. https://doi.org/10.1029/2012JD018332

Makvandi R, Maghsoodolkamali B, Mohammadfam I (2012) Utilization of TOPSIS multi-criteria decision making model in environmental impact assessment of oil refineries (case study: Khuzestan super heavy oil refinery). J Environ Res 3:77–86 [In Persian]

Meinander O, Kontu A, Virkkula A, Arola A, Backman L, Dagsson-Waldhauserová P et al (2014) Brief communication: light-absorbing impurities can reduce the density of melting snow. Cryosphere 8(3):991–995

Monika D, Outi M, Tinna J, Tobias D, Gerrit DL, Finnur P, Pavla DW, Throstur T (2016) Insulation effects of Icelandic dust and volcanic ash on snow and ice. Arab J Geosci 9:126. https://doi.org/10.1007/s12517-015-2224-6

Nabavi O, Haimberger L, Samimi C (2017) Sensitivity of WRF CHEM predictions to dust source function specification in West Asia. Aeolian Res 24:115–131

Naserpour S, Alijani B, Ziaeian P (2015) Source identification of dust hurricanes in the southwest of Iran using satellite images and aerial maps. Phys Geogr Res 1:36–21

Nazmfar H, Alibakhshi A (2014) Spatial inequality measurement in using educational indices using TOPSIS method (case study: Khozestan Province). J Educ Plan Stud 3:115–134 [In Persian]

Niu X, Pinker RT (2015) An improved methodology for deriving high-resolution surface shortwave radiative fluxes from MODIS in the Arctic region. J Geophys Res Atmosp 120:2382–2393. https://doi.org/10.1002/2014JD022151

Painter TH, Skiles SM, Deems JS, Bryant AC, Landry C (2012) Dust radiative forcing in snow of the upper Colorado River basin: part I. a 6 year record of energy balance, radiation, and dust concentrations. Water Resour Res. https://doi.org/10.1029/2012WR011985

Rafał D, Jan J, Mariusz H (2016) Physical and chemical characteristics of after-reclamation dust from used sand moulds. Arab J Geosci 9:153. https://doi.org/10.1007/s12517-015-2162-3

Safarianzengir V, Sobhani B, Asghari S (2019) Modeling and monitoring of drought for forecasting it, to reduce natural hazards atmosphere in western and north western part of Iran. Iran Air Qual Atmos Health 13:119–130. https://doi.org/10.1007/s11869-019-00776-8

Sahraei, J, Bahrami M, Mohammadi N (2017) Dust storm tracking (case study: Khuzestan). The first conference of Ideas and Technologies in geography 16–11. [In Persian]

Sahu O, Rao D, Gabbiye N, Engidayehu A, Teshale F (2017) Sorption of phenol fram synthetic aqueous solution by activated saw dust. Biochem Biophys Rep 12:46–53

Shamsipour AA, Safarrad T (2012) Synoptic satellite analysis of dust phenomena. Nat Geogr Res 44:126–111 [In Persian]

Shoji M, Kawamura G, Smirnov R, Pigarov A, Tanaka Y, Masuzaki S, Uesugi Y (2017) Simulation of impurity transport in the peripheral plasma due to the emission of dust in long pulse discharges on the large helical device. Nucl Mater Energy 12:779–785

Sobhani B, Safarian VZ (2019) Modeling, monitoring and forecasting of drought in south and southwestern Iran. Iran Model Earth Syst Environ 5:63–71. https://doi.org/10.1007/s40808-019-00655-2

Sobhani B, Safarian VZ, Kianian MK (2019b) Modeling, monitoring and prediction of drought in Iran. Iran (Iranica) J Energy Environ 10: 216–224. https://doi.org/10.5829/ijee.2019.10.03.09

Sobhani B, Safarian VZ, Kianian MK (2019a) Drought monitoring in the Lake Urmia basin in Iran. Arab J Geosci 12:448. https://doi.org/10.1007/s12517-019-4571-1

Sobhani B, Safarian VZ, Kianian MK (2018) Potentiometric mapping for wind turbine power plant installation Guilan Province in Iran. J Appl Sci Environ Manage 22:1363–1368. https://doi.org/10.4314/jasem.v22i8.36

Tohidi AH, Zaremehrjerdi MR, Mehrabi H, NezamAbadipour H (2015) Estimation of artificial neural network-data panel hybrid model in estimating Iran's dried fruits export prices. J Quant Econ 12:95–116 [In Persian]

Wang Z, Pan X, Uno I, Li J, Wang Z, Chen X, Fu P, Yang T, Kobayashi H, Shimizu A, Sugimoto N, Yamamotom S (2017) Significant impacts of heterogeneous reactions on the chemical composition and mixing state of dust particles. Atmos Environ 15:83–91

Willame Y, Vandaele AC, Depiesse C, Lefèvre F, Letocart V, Gillotay D, Montmessin F (2017) Retrieving cloud dust and ozone abundances

in the Martian atmosphere SPICAM/UV nadir spectra. Planet Space Sci 142:9–25

Woldridge JM (2006) Introductory econometrics: a modern approach, 3rd edn. South-Western, New York

Xinghua Z, HaifengW XC, Chaonan F, KunT XZ (2019) Experimental study on dust suppression at transhipment point based on the theory of induced airflow dust production. Build Environ 160:106–200. https://doi.org/10.1016/j.buildenv.2019.106200

Zalesna E, Grzonka J, Rubel M, Carrasco A, Widdowson A, Baron A, Ciupinski L, Contributors, Jet (2017) Studies of dust from JET with the ITER like wall: composition and internal structure. Nucl Mater Energy 12:582–587

Zielhofer C, Suchodoletz H, Fletcher W, Schneider B, Dietze E, Schleget M, Schepanski K, Weninger B, Mischke S, Mikdad A (2017) millennial scale fluctuations in Saharan dust supply across the decline of the African humid period. Quatemary Sci Rev 171:119–135

Zolfaghari H, Samakosh J, Shayganmehr SH, Ahmadi M (2011) A synoptic investigation of dust storms in western regions of Iran. J Geogr Environ Plan 43:17–34 [In Persian]